Ab initio theory of electron-phonon mediated ultrafast spin relaxation of laser-excited hot electrons in transition-metal ferromagnets

K. Carva,[1,2,*] M. Battiato,[1] D. Legut,[3] and P. M. Oppeneer[1]

[1]*Department of Physics and Astronomy, Uppsala University, P. O. Box 516, S-75120 Uppsala, Sweden*

[2]*Charles University, Faculty of Mathematics and Physics, Department of Condensed Matter Physics, Ke Karlovu 5, CZ-12116 Prague 2, Czech Republic*

[3]*Nanotechnology Centre, VSB-Technical University of Ostrava, 17. listopadu 15, CZ-708 33 Ostrava, Czech Republic*

(Received 22 February 2013; published 22 May 2013)

We report a computational theoretical investigation of electron spin-flip scattering induced by the electron-phonon interaction in the transition-metal ferromagnets bcc Fe, fcc Co, and fcc Ni. The Elliott-Yafet electron-phonon spin-flip scattering is computed from first principles, employing a generalized spin-flip Eliashberg function as well as *ab initio* computed phonon dispersions. Aiming at investigating the amount of electron-phonon mediated demagnetization in femtosecond laser-excited ferromagnets, the formalism is extended to treat laser-created thermalized as well as nonequilibrium, nonthermal hot electron distributions. Using the developed formalism we compute the phonon-induced spin lifetimes of hot electrons in Fe, Co, and Ni. The electron-phonon mediated demagnetization rate is evaluated for laser-created thermalized and nonequilibrium electron distributions. Nonthermal distributions are found to lead to a stronger demagnetization rate than hot, thermalized distributions, yet their demagnetizing effect is not enough to explain the experimentally observed demagnetization occurring in the subpicosecond regime.

DOI: 10.1103/PhysRevB.87.184425 PACS number(s): 78.47.J−, 78.20.Ls, 75.78.Jp, 78.20.Bh

I. INTRODUCTION

In recent years it has been demonstrated that magnetization can be changed without applying an external magnetic field in extremely short time scales of the order of hundreds of femtoseconds.[1–4] Although it initial appeared that this would not be possible using strong pulsed magnetic fields,[5] it was discovered that an ultrafast demagnetization of ferromagnetic transition metals could be induced by a femtosecond laser pulse.[1,6–8] A closely related but more complex process of optically induced magnetization switching has recently been discovered for ferrimagnetic systems with two antiparallel sublattice magnetizations.[9–11] These discoveries offer possible routes to manipulate the magnetic moment on a subpicosecond time scale and may lead to technological breakthrough in future ultrafast memory devices.

The observation of ultrafast all-optical demagnetization in elemental ferromagnets has led to an intensive and on-going debate on what actually is the microscopic origin of the ultrafast process.[4,12–16] A first proposal for a microscopic explanation was based on direct transfer of angular momentum from the light, assisted by the spin-orbit (SO) interaction.[17] Later, it was, however, argued quantitatively that this source of photon angular momentum is insufficient to cause such a huge observed demagnetization,[18] when taking into account the amount of photons present in the experiment and the estimated probability of a spin-flip (SF) excitation. It has subsequently been argued that the ultrafast magneto-optical Kerr effect (MOKE) response on the femtosecond time scale could be modified by existing nonequilibrium (NEQ) electron distribution created by the femtosecond pump laser,[18–21] yet this effect would disappear in a few hundred femtoseconds[22] and the MOKE signal would thereupon follow the time evolution of the magnetization dynamics. Hereafter, a number of theoretical models have been proposed to explain the ultrafast demagnetization; most of these are based on the assumption of a particular spin dissipation channel.[4,14,15,23–25] Ultrafast spin dissipation channels that have been put forward are Elliott-Yafet electron-phonon SF,[15,23] electron-magnon SF,[24,26] and electron-electron SF[25] scatterings; spin-orbit interaction is again the precursor in these electron-quasiparticle scatterings. Also, direct, laser-induced SF processes[14] and relativistic spin-light interaction[4] have been suggested. Further, a distinct model, which does not assume ultrafast spin-flips but instead fast, superdiffusive transport of spins carried away with hot electrons has been proposed.[27,28] A few first observations[29–32] of laser-induced spin transport have been reported recently.

Even when the origin of the ultrafast spin relaxation is not known, model simulations on the basis of the Landau-Lifshitz-Gilbert and Landau-Lifshitz-Bloch equations can provide valuable insight.[9,11,33–35] In these simulations, suitably chosen longitudinal SF dissipation and transversal damping parameters, due to an unspecified microscopic mechanism, are adopted. With well-chosen dissipation parameters, the measured laser-induced magnetization response can be captured, for elemental ferromagnets[35,36] and for ferrimagnets with two sublattice magnetizations.[10,11,37,38] The achieved correspondence with the measured ultrafast spin-dynamics may have implications for unveiling the ultrafast spin-flip channel. For example, on the basis of Landau-Lifshitz-Bloch simulations, it was recently argued, for the laser-induced demagnetization in Gd, that phonon-mediated spin flips are needed above the Debye temperature, whereas below it electron-electron SF interaction should be sufficient.[39]

The phonon-mediated Elliott-Yafet SF scattering has recently received significant attention.[15,23] On the basis of the Elliott-Yafet theory (in the Elliott spin-mixing approximation),[40] a unification of the theory of ultrafast demagnetization with the theory of Gilbert damping has been suggested.[41–43] Moreover, strong arguments in favor of the Elliott-Yafet SF scattering as a dominant mechanism for ultrafast laser-induced demagnetization were presented by

Koopmans *et al.*[15] Experimentally fitted SF probabilities were in reasonably good agreement with theoretical SF probabilities that were computed *ab initio* using the Elliott spin-mixing approximation.[44] A large effective demagnetization was found when these SF probabilities were employed in the microscopic three temperature model (M3TM).[15] Elliott-Yafet SF scattering combined with the M3TM has furthermore predicted correctly the observed relation between the demagnetization rates in Ni, Co, and Gd,[15] but these calculations rest on a number of approximations and contain a fitting parameter for each calculated metal. The measured temperature dependence of the laser-induced magnetization dynamics was consistent with the phonon-mediated spin dissipation.[45]

Although these results might provide support for the Elliott-Yafet phonon-mediated processes as mechanism underlying ultrafast demagnetization, first-principles investigations have to be performed to quantify more precisely the amount of demagnetization that can be achieved by electron-phonon SF scattering. Recently, the first *ab initio* investigations have been undertaken,[46,47] yet more such investigations, considering different materials are required to obtain a complete picture.

To calculate the demagnetization rate created by Elliott-Yafet electron-phonon processes, two major steps have to be performed. The first one is to evaluate the SF probability during a scattering event, which is assumed to be the origin of the spin magnetization dissipation. This step is clear from the theory point of view and the difference between methods of various groups lies mainly in how detailed the description of scattering is, e.g., at the level of inclusion of real phonon dispersions and evaluation of the electron-phonon matrix elements (cf. Refs. 43,44,46, and 47). The second step is the calculation of the actual demagnetization rate employing the calculated SF probabilities. In this step, several assumptions may come into play. One of these, is the treatment of the laser-excited electron and spin systems and their thermalization. On the initial femtosecond time scale, after irradiation, the electron system is not in equilibrium with neither the lattice nor the spin system. Note that the laser irradiation must be very intensive to cause observable demagnetization, hence a significant amount of electrons is excited during the process to high-energy levels. The proper inclusion of this nonequilibrium situation might well be crucial for correctly modeling the ultrafast demagnetization. The occurring NEQ distributions also represent a complication for measurements of the spin dynamics on the femtosecond time scale, which are commonly performed utilizing MOKE[18,48,49] or the x-ray magnetic circular dichroism (XMCD),[10,50,51] as the redistribution of electrons has to be taken into account when interpreting experimental data.[16,19,21,52] The laser-generated electron and spin distributions have, however, been modeled in rather different ways recently.[15,44,46,47] Sometimes, only a thermalized electron distribution has been assumed,[15] or the presence of laser-excited states has been approximated by averaging over a large energy interval.[44]

Here, we aim at developing a theoretical treatment for accurately calculating electron-phonon generated ultrafast spin relaxation without employing the approximate Elliott relation. Our treatment is based on a generalized spin- and energy-dependent Eliashberg function[53] and involves a new quantity, the SF probability as a function of electron energy. The computational scheme has been implemented in a relativistic *ab initio* band-structure code, and hence it does not rely on assumptions regarding the shape of the spin-polarized density of states (DOS). Importantly, our computational approach is valid not only for thermalized electron distributions, but also for the more general nonthermal distributions that are expected to exist in the material within the first 300 fs after the pump pulse. Using the developed formalism, we investigate the phonon-induced SF rates and spin dynamics of the ferromagnetic transition metals Fe, Co, and Ni, treating both thermalized as well as nonthermalized hot electron distributions. Our calculated demagnetization rates shed promptly more light on the mechanism of ultrafast magnetization dynamics. In particular, we find that nonthermal electron distributions lead to a stronger demagnetization rate than thermal electron distributions, however, the contribution of phonon-induced SF scattering is not sufficient to explain the measured ultrafast demagnetization.

II. THEORY

Within electron band theory, spin nonconserving processes in ferromagnetic crystalline solids arise from the spin-orbit interaction. In the presence of the SO interaction, the majority and minority Bloch eigenstates $|\Psi^{\uparrow}_{\boldsymbol{kn}}\rangle$ and $|\Psi^{\downarrow}_{\boldsymbol{kn}}\rangle$ can be decomposed into spin-up and spin-down spinor parts,

$$|\Psi^{\uparrow}_{\boldsymbol{kn}}\rangle = a^{\uparrow}_{\boldsymbol{kn}}|\Uparrow\rangle + b^{\uparrow}_{\boldsymbol{kn}}|\Downarrow\rangle\,, \quad |\Psi^{\downarrow}_{\boldsymbol{kn}}\rangle = a^{\downarrow}_{\boldsymbol{kn}}|\Downarrow\rangle + b^{\downarrow}_{\boldsymbol{kn}}|\Uparrow\rangle. \quad (1)$$

The spinor components $b^{\sigma}_{\boldsymbol{kn}}$ ($\sigma = \uparrow,\downarrow$) are generally small (compared to $a^{\sigma}_{\boldsymbol{kn}}$) and nonzero only if SO coupling is present. They represent the degree of SO-induced spin mixing.

In the following, we first describe the theory for electron-phonon generated spin-flip scattering in thermal equilibrium at low temperatures. Subsequently, we extend the formalism to treat SF scattering for situations out of the low-temperature equilibrium.

A. Phonon induced spin flips in equilibrium

An accurate calculation of the electron-phonon SF scattering has to be based on the phonon spectrum $\omega_{\boldsymbol{q}\nu}$ and the electron-phonon matrix elements[54] $g^{\nu}_{\boldsymbol{kn},\boldsymbol{k}'n'}(\boldsymbol{q})$. Here, ν and $\boldsymbol{q}$ denote the phonon mode and wave vector and $\boldsymbol{kn}$, $\boldsymbol{k}'n'$ are the electron quantum numbers; momentum conservation demands $\boldsymbol{q} = \boldsymbol{k}' - \boldsymbol{k}$. The (squared) spin-resolved electron-phonon matrix elements $g^{\nu\sigma\sigma'}_{\boldsymbol{kn},\boldsymbol{k}'n'}(\boldsymbol{q})$ are defined by

$$g^{\nu\sigma\sigma'}_{\boldsymbol{kn},\boldsymbol{k}'n'}(\boldsymbol{q}) = \left|\boldsymbol{u}_{\boldsymbol{q}\nu}\cdot\left\langle\Psi^{\sigma}_{\boldsymbol{kn}}\middle|\nabla_{\boldsymbol{R}}V\middle|\Psi^{\sigma'}_{\boldsymbol{k}'n'}\right\rangle\right|^2, \quad (2)$$

where V is the total potential felt by the electrons, $\boldsymbol{u}_{\boldsymbol{q}\nu}$ is the phonon polarization vector, and $\nabla_{\boldsymbol{R}}$ denotes the gradient with respect to the displacements of the atoms,[54,55] which correspond to the mode $\boldsymbol{u}_{\boldsymbol{q}\nu}$.

To derive a suitable low-temperature formulation, we consider which electronic states $|\Psi^{\sigma}_{\boldsymbol{kn}}\rangle$ can participate in the scattering. Energy conservation in the electron-phonon scattering dictates the condition $\delta(E^{\sigma'}_{\boldsymbol{k}'n'} - E^{\sigma}_{\boldsymbol{kn}} - \hbar\omega_{\boldsymbol{q}\nu})$. At zero temperature, electronic states up to the Fermi energy E_F are occupied, therefore conduction electrons with energies $E^{\sigma}_{\boldsymbol{kn}}$ in the range $[E_F - \hbar\Omega,\ E_F]$ are allowed to absorb a

phonon with energy Ω. The energy of the final state $E^{\sigma'}_{\boldsymbol{k}'n'}$ then lies in the range $[E_F,\ E_F+\hbar\Omega]$. If one can neglect the difference in the electronic states that differ by an energy Δ that is smaller than the maximum phonon energy $\hbar\omega_{\max}$ (i.e., $E^{\sigma}_{\boldsymbol{k}n}$ and $E^{\sigma}_{\boldsymbol{k}n}+\Delta$), a suitable approximation can be made. It is customary to describe the distribution of states with energy E participating in the scattering by a δ function broadened by a width Δ, denoted by $\tilde{\delta}(E-E_F)$. Such broadening is also needed for numerical implementation of formulas involving δ functions. Note that maximal phonon frequencies are typical of about 35 meV and the broadening of the electron distribution is already 25 meV at room temperature. Consequently, we can write the condition for the initial and final states together with the requirement for energy conservation in a symmetrical form: $\tilde{\delta}(E^{\sigma}_{\boldsymbol{k}n}-E_F)\tilde{\delta}(E^{\sigma'}_{\boldsymbol{k}'n'}-E_F)$. The approximation to ignore the distinction between conduction electron states differing by less than the maximum phonon energy was already made in earlier works.[54,56]

The next step to describe the electron-phonon scattering is to introduce the equilibrium Eliashberg function.[54] The standard, spin-diagonal equilibrium Eliashberg function is obtained when the squared electron-phonon matrix elements are integrated over all possible initial and final electronic states, restricted by the phonon energy ($\Omega=\omega_{\boldsymbol{q}\nu}$) as a parameter.[54] For our purpose, it is necessary to define a spin-dependent equilibrium Eliashberg function $\alpha^2_{\sigma\sigma'}F^0(\Omega)$, resolved with respect to the spin state of initial and final states, which reads

$$\alpha^2_{\sigma\sigma'}F^0(\Omega)=\frac{1}{2M\Omega}\sum_{\nu,n,n'}\int d\boldsymbol{k}\int d\boldsymbol{k}'\,g^{\nu\sigma\sigma'}_{\boldsymbol{k}n,\boldsymbol{k}'n'}(\boldsymbol{q}=\boldsymbol{k}'-\boldsymbol{k})\times\delta(\omega_{\boldsymbol{q}\nu}-\Omega)\tilde{\delta}\big(E^{\sigma}_{\boldsymbol{k}n}-E_F\big)\tilde{\delta}\big(E^{\sigma'}_{\boldsymbol{k}'n'}-E_F\big). \tag{3}$$

The spin-flip processes are given by the terms with $\sigma\neq\sigma'$, hence, the equilibrium SF Eliashberg function is given by $\alpha^2_{\uparrow\downarrow}F^0(\Omega)$.[56] The sum over diagonal elements $\sigma=\sigma'$ corresponds to the standard Eliashberg function, $\alpha^2F^0(\Omega)$. Characteristic features of the electron-phonon scattering, which are important for the evaluation of Eq. (3), are the facts that the change in electron energy is small, typically below 40 meV, but any momentum change in the scattering process is possible.

As long as one is not interested in knowledge about electron-phonon scattering contributions stemming from specific phonons, it is useful to integrate over all phonon energies and obtain the spin-resolved transition rate $w^0_{\sigma\sigma'}$,

$$w^0_{\sigma\sigma'}=\int_0^{\omega_{\max}}d\Omega\,\alpha^2_{\sigma\sigma'}F^0(\Omega)\,[1+2N(\Omega)], \tag{4}$$

where $N(\Omega)$ is the phononic Bose-Einstein distribution function. Analogously, one can define the total transition rate w^0 (which in the current formulation includes *both* spin-diagonal and nondiagonal scattering events). Lastly, one can introduce the total SF probability P_S, which is defined as the ratio of the SF and total scattering rates,

$$P_S=\frac{w^0_S}{w^0}. \tag{5}$$

B. Laser-irradiated ferromagnets

To approach further the physical situation, which is in the focus of the present study, we need to examine electron-phonon spin-flip scattering in laser-heated ferromagnets. Due to the pump-laser excitation and the subsequent process of electron thermalization, not only electron states in the immediate vicinity of the Fermi energy will be involved, also energetically deep-lying states that are reached by the pump laser as well as states at higher energies above E_F that become populated have to be taken into account.

Following the above derivation, it is straightforward to define a generalized spin- and energy-dependent Eliashberg function,

$$\alpha^2_{\sigma\sigma'}F(E,\Omega)=\frac{1}{2M\Omega}\sum_{\nu,n,n'}\int d\boldsymbol{k}\int d\boldsymbol{k}'\,g^{\nu\sigma\sigma'}_{\boldsymbol{k}n,\boldsymbol{k}'n'}(\boldsymbol{q})\delta(\omega_{\boldsymbol{q}\nu}-|\Omega|)\times\delta\big(E^{\sigma}_{\boldsymbol{k}n}-E\big)\delta\big(E^{\sigma'}_{\boldsymbol{k}'n'}-E^{\sigma}_{\boldsymbol{k}n}-\hbar\Omega\big). \tag{6}$$

A negative Ω is possible and allowed (for absorption processes). As we are interested in the regime of the order of hundreds of femtoseconds after the laser pulse, we can assume that the lattice has not yet been heated up and therefore the room temperature phonon distribution $N(\Omega)$ is assumed. This assumption is substantiated by recent measurements showing a rise of the lattice temperature of Ni in a few picoseconds after laser excitation, which is much slower than the ultrafast demagnetization.[57]

In a laser-pumped system, the electrons are redistributed depending on the laser frequency and the amount of absorbed radiation. The electronic system can be described by suitably modified distribution functions.[21,52,58] Also here, we describe this redistribution by band-index independent occupation factors $f_\sigma(E)$, thus catching the key quantities of the laser-pumped electron system—its spin and energy dependence. The assumption that all states labeled by σ and E have the same occupancy is partially justified by the simple band structure of the studied metals in the region above E_F. We note that it is possible to go beyond this approximation with the presented formalism, but at the cost of significant numerical complications. Using this approximation, the spin-resolved transition rate,[59] which is the key quantity for magnetization evolution, is defined as

$$S^{\sigma\sigma'}=\iint d\Omega dE\,\alpha^2_{\sigma\sigma'}F(E,\Omega)f_\sigma(E)\times[1-f_{\sigma'}(E+\hbar\Omega)][\Theta(\Omega)+N(\Omega)]. \tag{7}$$

The main goal of this study is to determine the total temporal evolution of spin moment. In order to understand the relation between the spin evolution and typical electron distributions occurring after the laser pulse, we reformulate the above expressions using phonon-integrated quantities. This is done at the cost of neglecting the difference between $f_\sigma(E)$ and $f_\sigma(E+\hbar\Omega)$, and the difference between the electron-phonon matrix elements of states with energies $E^{\sigma}_{\boldsymbol{k}n}$ and $E^{\sigma}_{\boldsymbol{k}n}+\hbar\Omega$. The latter approximation is a complete analogy to the one made above in deriving the equilibrium Eliashberg function $\alpha^2_{\sigma\sigma'}F^0(\Omega)$. It is a plausible approximation because the phonon energy is much lower than the range of electron energies made available due to the pump laser, or the energy on which the

band structure would be significantly changed. The results obtained with this approximation have been checked against calculations using the accurate Eq. (7) for the case of Ni.

This approximation allows to neglect Ω in $\delta(E_{k'n'} - E_{kn} - \hbar\Omega)$, when simultaneously the δ function is replaced by its broadened counterpart, $\tilde{\delta}$. This leads to a reformulation of the Eliashberg function similar to the one made in the equilibrium case, specifically,

$$\alpha^2_{\uparrow\downarrow}F(E,\Omega) \simeq \frac{1}{2M|\Omega|}\sum_{\nu,n,n'}\int d\boldsymbol{k}\int d\boldsymbol{k}' g^{\nu\uparrow\downarrow}_{\boldsymbol{k}n,\boldsymbol{k}'n'}(\boldsymbol{q}) \times \delta(\omega_{\boldsymbol{q}\nu} - |\Omega|)\tilde{\delta}(E^{\uparrow}_{\boldsymbol{k}n} - E)\tilde{\delta}(E^{\downarrow}_{\boldsymbol{k}'n'} - E). \quad (8)$$

Next, to achieve a further rewriting of the equations, we investigate how the generalized Eliashberg functions for spin-majority to spin-minority scattering and *vice versa* are related. To this end, we note that upon interchanging $\boldsymbol{k} \leftrightarrow \boldsymbol{k}'$ in the integration and employing $g^{\nu\sigma\sigma'}_{\boldsymbol{k}n,\boldsymbol{k}'n'}(\boldsymbol{q}) = g^{\nu\sigma'\sigma}_{\boldsymbol{k}'n',\boldsymbol{k}n}(\boldsymbol{q})$, we obtain

$$\begin{aligned}\alpha^2_{\uparrow\downarrow}F(E,\Omega) &= \frac{1}{2M|\Omega|}\sum_{\nu,n,n'}\int d\boldsymbol{k}\int d\boldsymbol{k}' g^{\nu\downarrow\uparrow}_{\boldsymbol{k}n,\boldsymbol{k}'n'}(\boldsymbol{q}) \\ &\quad\times \delta(\omega_{\boldsymbol{q}\nu} - |\Omega|)\tilde{\delta}(E^{\downarrow}_{\boldsymbol{k}n} - E)\tilde{\delta}(E^{\uparrow}_{\boldsymbol{k}'n'} - E) \\ &= \alpha^2_{\downarrow\uparrow}F(E,\Omega). \end{aligned} \quad (9)$$

Hence, the equivalence $\alpha^2_{\uparrow\downarrow}F(E,\Omega) = \alpha^2_{\downarrow\uparrow}F(E,\Omega)$ is proven. The approximation to neglect the influence of Ω on the energies while broadening the δ function also elevates the need for distinguishing a negative Ω, since the difference between phonon absorption and emission becomes negligible and $\alpha^2_{\uparrow\downarrow}F(E,\Omega) \approx \alpha^2_{\uparrow\downarrow}F(E,-\Omega)$.

We can now define $w_{\sigma\sigma'}(E)$, which is a generalization of the above-defined $w^0_{\sigma\sigma'}$, i.e., a spin- and energy-dependent scattering rate that involves the average over all available states at a given energy E and all phonon states (or equivalently, all destination states),

$$w_{\sigma\sigma'}(E) = \int_0^\infty d\Omega\, \alpha^2_{\sigma\sigma'}F(E,\Omega)\,[1 + 2N(\Omega)]\,. \quad (10)$$

Consequently, the spin-resolved transition rates are

$$S^{\sigma\sigma'} = \int dE\, w_{\sigma\sigma'}(E) f_\sigma(E)[1 - f_{\sigma'}(E)]. \quad (11)$$

Apparently, we obtain $w_{\uparrow\downarrow}(E) = w_{\downarrow\uparrow}(E) = w_S(E)$, because the same expression is valid for $\alpha^2_{\uparrow\downarrow}F(E,\Omega)$. Therefore we can introduce the spin *decreasing* transition rate $S^- = S^{\uparrow\downarrow}$ and the spin *increasing* rate $S^+ = S^{\downarrow\uparrow}$, which are given by formulas that differ only through the occupation factors,

$$\begin{aligned} S^- &= \int dE\, w_S(E) f_\uparrow(E)\,[1 - f_\downarrow(E)], \\ S^+ &= \int dE\, w_S(E) f_\downarrow(E)\,[1 - f_\uparrow(E)]. \end{aligned} \quad (12)$$

Employing this formulation, the temporal evolution of the spin moment can be connected with the (nonequilibrium) electron distributions that are typically expected to occur in laser-excited ferromagnets. The total electron-phonon scattering rate is given simply as $w(E) = \sum_{\sigma\sigma'} w_{\sigma\sigma'}(E)$. The SF probability for an electron at a given energy E during an electron-phonon scattering can be defined as $p_S(E) = w_S(E)/w(E)$. The total SF probability for a system with electron occupancies described by a distribution $f_\sigma(E)$ is

$$P_S = (S^- + S^+)/\sum_{\sigma\sigma'} S^{\sigma\sigma'}. \quad (13)$$

Importantly, the crucial quantity for demagnetization is the demagnetization rate, which arises as the balance of spin-increasing and spin-decreasing spin-flip scatterings. It is given by $dM/dt = 2\mu_B(S^- - S^+)$, where M is the z component of the spin moment. Note that we consider here the initial demagnetization $dM/dt(t = 0)$ in a first-order approximation, which allows us to compare to measured demagnetization rates, $dM/dt(0) = -[M(0) - M_{\min}]/\tau_M$, with $M_{\min}$ being the achieved minimal magnetization. A higher-order magnetization change induced by a reduction of the exchange field is not taken into account.

Lastly, we also define a relative quantity called demagnetization ratio, by taking the difference between spin decreasing and increasing transition processes but normalized to the total transition rate:

$$D_S = (S^- - S^+)/\sum_{\sigma\sigma'} S^{\sigma\sigma'}. \quad (14)$$

C. The Elliott relation

As the evaluation of the spin-dependent electron-phonon matrix elements is a demanding computational step, several approximations have been introduced in the past. One of these is the Elliott approximation, which we describe here in more detail as it was used in recent theoretical works to explain the ultrafast laser-induced demagnetization[15,44] as well as the ultrafast magnetic phase transition occurring in FeRh.[60] This approximation is not used in our model, only, we have computed some results based on it (denoted as Elliott SF probability), which are shown in graphs for the sake of comparison.

Elliott[40] originally pointed out that even the spin-diagonal part of the potential V can connect eigenstates of majority and minority spin because of the spin-mixing present in the eigenstates, thus effectively allowing for a spin-flip scattering. Making several approximations, Elliott could derive a relation between the spin lifetime τ_{SF} for a general kind of scattering event that has a spin-diagonal lifetime τ. The employed assumptions are that the material is a paramagnetic metal, the variations of the electron-phonon matrix elements over the Brillouin zone (BZ) are small, $b_{\boldsymbol{k}n}$ is constant over the BZ, and $b^\sigma_{\boldsymbol{k}n} \ll a^\sigma_{\boldsymbol{k}n}$.[40,53] The resulting relation called after Elliott employs the Fermi-surface averaged spin mixing of eigenstates,

$$\langle b^2\rangle = \sum_{\sigma,n}\int d\boldsymbol{k}\left|b^\sigma_{\boldsymbol{k}n}\right|^2\tilde{\delta}\left(E^\sigma_{\boldsymbol{k}n} - E_F\right), \quad (15)$$

and predicts the SF probability $P^{b^2}_S$ to be approximately

$$P^{b^2}_S = \frac{\tau}{\tau_{\text{SF}}} = 4\langle b^2\rangle. \quad (16)$$

The Elliott relation can also be generalized to nonequilibrium situations.[46] To this end, we define a SF density of states as an averaged b^2 component of all states at a given energy E,

in analogy to the usual definition of the total DOS $n(E)$:

$$n_{\uparrow\downarrow}(E) = \sum_{\sigma,n} \int d\boldsymbol{k} \left|b^{\sigma}_{\boldsymbol{k}n}\right|^2 \delta\left(E^{\sigma}_{\boldsymbol{k}n} - E\right). \tag{17}$$

Applying the Elliott approximation for one electron at energy E, we obtain an energy-resolved SF probability $p_S^{b^2}(E) = 4\langle b^2\rangle(E) = 4n_{\uparrow\downarrow}(E)/n(E)$.

Analogous to the expressions in the preceding section, the total Elliott SF probability $P_S^{b^2}$ of an electron system after laser excitation can be computed by adopting a representative electron distribution $f_\sigma(E)$ and performing an energy integration similar to the one in Eq. (11). To this end, $w_{\uparrow\downarrow}(E)$ has to be replaced by $n_{\uparrow\downarrow}(E)$ and $w(E)$ by $n(E)$. The total Elliott SF probability follows from an expression equivalent to Eq. (13).

The Elliott relation was originally intended to treat electron-phonon scattering, but because of the approximations made, it does no longer rely on any phonon characteristics of the scattering. Therefore the Elliott SF probability would be the same irrespective if the SF scattering is due to phonons or, e.g., defects.

Apart from the spin-mixing in the wave functions, a different SF scattering can arise from the spin-orbit coupling part of the potential V_{SO}, as originally proposed by Overhauser.[61] Yafet[59] showed that, at low temperatures, the contribution of this term to the SF scattering almost cancels the spin-mixing contribution of Elliott (see also Ref. 56). Notwithstanding, experimental investigations[62] for nonmagnetic metals indicated that the trend given by Elliott's relation remained approximately valid, up to a multiplication with a materials specific constant within a variation of roughly one order of magnitude, but larger deviations were also reported for some metals.[62]

An essential assumption made in the derivation of Elliott's relation, which is relevant for the discussion of ultrafast demagnetization in ferromagnets, is that the material treated is a nonmagnetic metal, i.e., the scattering electron from initial state $|\boldsymbol{k}n\rangle$ can undergo a spin flip and goes back to the same spin-degenerate $|\boldsymbol{k}n\rangle$ as a final state. In spite of this, the Elliott relation has been applied to ferromagnetic metals,[15,44] but a recent investigation showed that it does fail for ferromagnetic metals with strongly exchange-split bands.[46] The obvious reason for this is that in exchange-split ferromagnetic bands the SF scattering electron has to go to a different final band state, which has a spin different from the original one.

D. Numerical implementation

The above derived equations for the electron-phonon SF scattering have been implemented within a first-principles band structure code. The electronic structure calculations are based on the density functional theory (DFT) and performed with the local spin density approximation (LSDA).[63,64] The full-potential linearized augmented plane wave (FP-LAPW) method for the electronic structure calculations is used because of its ability to describe phonons with high accuracy. We find that the calculated phonon dispersions of Ni and Fe are in reasonable agreement with other *ab initio* calculations and with experimental data.[65] The electron-phonon coupling elements are calculated self-consistently[55] within the ELK FP-LAPW code (http://elk.sourceforge.net/), hence $\nabla_{\boldsymbol{R}} V$ is evaluated for each $\boldsymbol{q}$ inside a supercell commensurate with $\boldsymbol{q}$. The calculations of the spin-resolved equilibrium Eliashberg function [see Eq. (3)] and its nonequilibrium counterpart [see Eq. (8)], the energy-dependent SF rate as well as the Elliott spin-mixing ratio have been implemented and are thus made available for the future study of a wide variety of metals. For systems with a complex band structure like transition metals and heavier elements, a good mesh density in reciprocal space is needed in order to obtain good BZ averages. On the other hand, high $\boldsymbol{k}$-space density of coupling elements requires big supercells, which makes calculations numerically demanding even for simple Ni. Here, we have used a $4 \times 4 \times 4$ mesh of phonon $\boldsymbol{q}$ points. As a test of our numerical implementation, we have calculated the SF and non-SF Eliashberg function of Al in equilibrium. These were found to be in good agreement with previous calculations,[56] with the SF Eliashberg function being approximately 10^5 times smaller than the non-SF Eliashberg function.

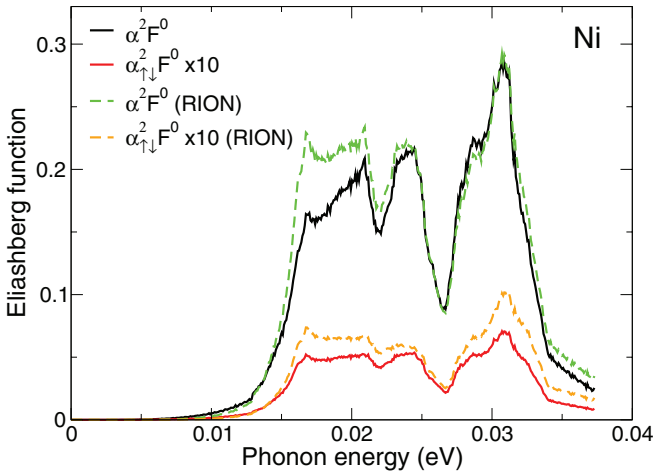

FIG. 1. (Color online) *Ab initio* calculated spin-flip Eliashberg $\alpha^2_{\uparrow\downarrow}F^0(\Omega)$ and total Eliashberg $\alpha^2F^0(\Omega)$ functions as a function of phonon energy Ω for Ni in equilibrium. For comparison, the SF and total Eliashberg functions computed with the rigid ion approximation (labeled with RION) are also given.

III. RESULTS

Our *ab initio* computed results for the elemental $3d$ ferromagnets are presented in the following. First, the generalized spin- and energy-dependent Eliashberg functions and scattering rates are given. For Ni, we, in addition, compare our calculated results with those obtained by two different approximations: the rigid-ion approximation by Nordheim[66] and an approximation introduced by Wang *et al.*[67] Subsequently, we present computed electron-phonon induced spin lifetimes of hot, nonthermal electrons and our results for phonon-mediated demagnetization in laser-excited $3d$ ferromagnets.

A. *Ab initio* SF probabilities and SF scattering rates

1. *fcc* Ni

The key information for examining the electron-phonon spin-flip probability for Ni in equilibrium at low temperatures ($<$300 K) is given by the equilibrium SF Eliashberg function (as compared to the total or non-SF Eliashberg function). In Fig. 1, we show the calculated SF and total Eliashberg

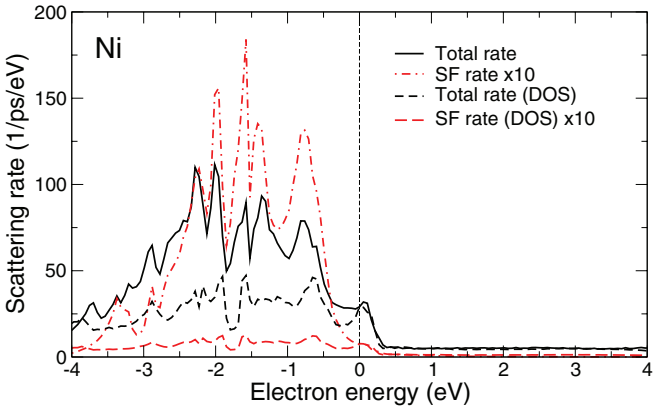

FIG. 2. (Color online) Energy-resolved electron-phonon total and SF scattering rates $w(E)$ and $w_S(E)$ for Ni obtained from direct *ab initio* calculations. For comparison, their counterparts obtained from the Ni DOS employing the approximation of Wang *et al.*[67] are also shown.

functions. The SF Eliashberg function is about 50 times smaller than its non-SF counterpart. As a result, as will be discussed below, the corresponding total SF probability P_S in equilibrium Ni [see Eq. (5)] is of the order of 10^{-2}.

In Fig. 1, we include results computed with the rigid ion approximation.[66] In this approximation, the total electron-lattice potential $V(\boldsymbol{r},\{\boldsymbol{R}_i\})$ is written as a superposition of on-site potentials $v(\boldsymbol{r}-\boldsymbol{R}_i)$ and for small core displacements it is assumed that the potential follows rigidly the motion of nuclei.[54,66] The rigid ion approximation is convenient to be used in conjunction with the atomic sphere approximation in band-structure calculations; recently, it was applied to study electron-phonon interaction in optically excited metals.[47] Here, we observe that the correspondence between the unapproximated Eliashberg functions and those obtained with the rigid-ion approximation is surprisingly good. All detailed structures in the functions are present, with at the most a difference in their amplitude. This suggests that the rigid-ion approximation could be used to achieve accurate SF probabilities.

To treat laser-heated ferromagnets, we need to include in the study the behavior of electrons away from the Fermi level. We thus consider the energy-resolved SF and non-SF scattering rates, $w_S(E)$ and $w(E)$; the calculated scattering rates are shown in Fig. 2. Near the Fermi energy, the phonon-induced SF rate is about 50 times smaller than the total rate, consistent with the behavior of the equilibrium SF and non-SF Eliashberg functions. At energies deeper below E_F, the SF scattering rate is only up to ten times smaller. Consequently, it can already be expected that, when electrons up to about 1.55 eV below E_F are affected by the laser excitation, the effective SF probability can increase considerably beyond the equilibrium SF probability.

Wang *et al.*[67] have proposed an approximation to avoid the tedious calculation of the energy-dependent Eliashberg function. This approximation entails using the equilibrium Eliashberg function scaled by the DOS, i.e.,

$$\alpha^2_{\sigma\sigma'}F(E,\Omega) \approx \alpha^2_{\sigma\sigma'}F^0(\Omega)\frac{n(E_F)}{n(E)}. \qquad (18)$$

This approximation was used in a previous computational investigation of the NEQ electron-phonon coupling in Ni.[68] From our calculations of $\alpha^2_{\sigma\sigma'}F(E,\Omega)$, we can easily undertake a verification of this approximation. The approximate energy-dependent Eliashberg function as predicted by Wang *et al.*'s formula is shown, too, in Fig. 2. Around the Fermi energy, the approximation is reasonable, as expected. However, at energies of more than 0.5 eV below E_F, the approximation becomes worse; the total electron-phonon scattering rate is predicted to be about a factor 2 too small by Wang *et al.*'s formula. The use of this formula appears to be especially insufficient for studying the spin-flip scattering rate, which is off by more than an order of magnitude.

The energy-dependent SF probability $p_S(E)$ as well as Elliott's SF probability $p^{b^2}_S(E)$ have been computed[46] recently for Ni, and are therefore not shown here. It was noted that both SF probabilities showed strong variations with electron energy, particular in the range of the d bands. Furthermore, the SF probability obtained from Elliott's relation could deviate a factor 2 to 3 from the directly computed SF probability. This deviation has been explained by the fact that Elliott's relation was originally derived for paramagnetic metals, where the same states are equally available to both spins, and a spin-flipping electron can, in each $\boldsymbol{k}$ point, scatter back to the same state. This assumption is, however, only poorly fulfilled in ferromagnets with strongly exchange-split bands.[46]

2. *bcc* Fe

The *ab initio* calculated SF and total Eliashberg functions of bcc Fe are shown in Fig. 3. Here, both the SF and total Eliashberg functions are more concentrated in a narrow peak area as compared to the case of Ni (cf. Fig. 1). The SF function is about 40 times smaller than the total Eliashberg function.

The calculated energy-resolved electron-phonon SF and total scattering rates are shown in Fig. 4 (top). The SF scattering rates are again about a factor of ten smaller than the non-SF scattering rates. In comparison to Ni, both scattering rates display more structure above E_F. In Fig. 4 (bottom), we show the computed electron-phonon SF probability $p_S(E)$ as well as the SF probability $p^{b^2}_S(E)$ obtained from the Elliott relation. These contain a few distinct features that differentiate

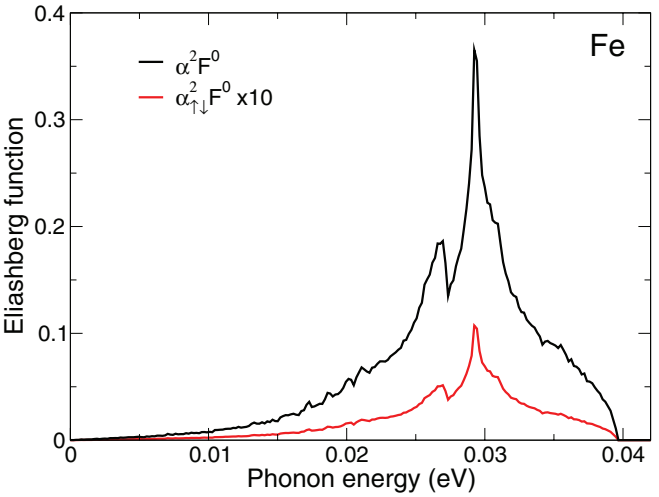

FIG. 3. (Color online) *Ab initio* calculated SF Eliashberg $\alpha^2_{\uparrow\downarrow}F^0(\Omega)$ and total Eliashberg $\alpha^2F^0(\Omega)$ functions of bcc Fe in equilibrium.

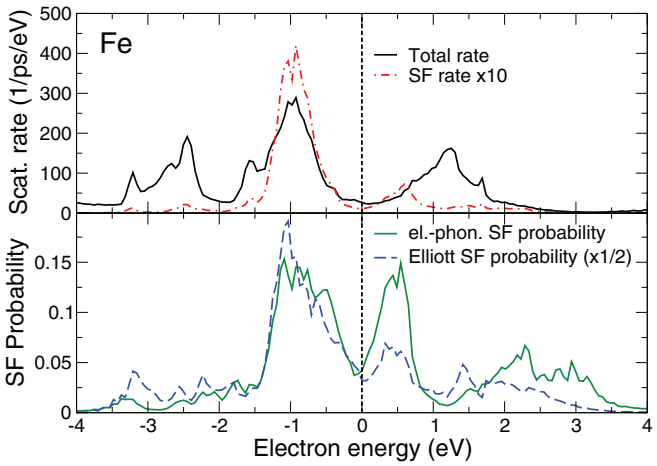

FIG. 4. (Color online) (Top) Calculated energy-resolved total and SF electron-phonon scattering rates, $w(E)$ and $w_S(E)$, of Fe. (Bottom) Calculated energy-resolved SF probability $p_S(E)$, and the approximate SF probability $p_S^{b^2}(E)$ (divided by two) obtained from Elliott's relation.

Fe from Ni, namely, the presence of an SF probability peak above the Fermi level, with a value of over 0.1. Also, the electron-phonon coupling is overall stronger in Fe than in Ni in the relevant range of ± 1.55 eV around the Fermi level by a factor of 2, while the difference of the SF probabilities of Fe and Ni at their Fermi levels is small. As all energy-dependent quantities vary strongly in the -1.55 to $+1.55$ eV region, the use of only Fermi level quantities to compute laser-induced demagnetization would be a very poor approximation. It is also worthwhile to note that the SF probability $p_S^{b^2}(E)$ obtained with the Elliott approximation is a factor of two larger than the directly computed SF probability for energies to -2 eV below the Fermi energy, whereas it is about the same size in the peak at 0.5 eV.

3. *fcc* Co

The *ab initio* calculated SF and total Eliashberg functions of fcc Co are shown in Fig. 5. Both the total and SF Eliashberg

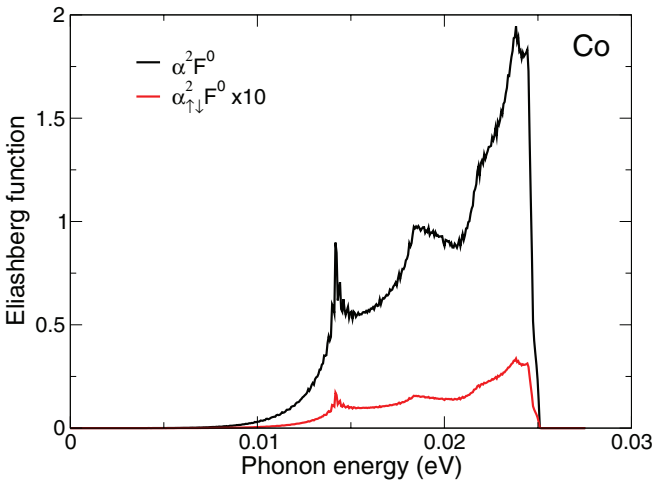

FIG. 5. (Color online) *Ab initio* calculated SF and total Eliashberg functions of fcc Co in equilibrium, as a function of the phonon energy.

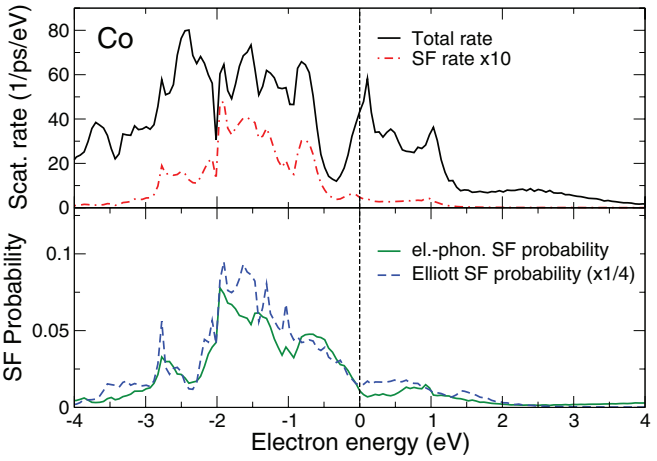

FIG. 6. (Color online) (Top) *Ab initio* calculated energy-resolved total and SF electron-phonon scattering rates of fcc Co. (Bottom) Calculated energy-resolved SF probability $p_S(E)$ as well as the approximate SF probability $p_S^{b^2}(E)$ (divided by four) obtained from Elliott's relation.

functions of Co exhibit overall higher values than those of the other two $3d$ ferromagnets, indicating a stronger electron-phonon coupling just at the Fermi level. However, the ratio of the SF to the total Eliashberg function is somewhat lower.

The calculated energy-resolved electron-phonon scattering rates and SF probabilities of Co are given in Fig. 6. The SF scattering rate around E_F is here particularly smaller than in Fe and Ni, whereas the shape of the energy-dependent SF rate is intermediate to those of Ni and Fe, with a smaller peak above the Fermi level. We further note that the total electron-phonon scattering rate exhibits a deep minimum below E_F and maximum above it—features that do not simply correspond to the total DOS. The directly computed energy-resolved SF probability (Fig. 6, bottom) is lower than in Ni and Fe; this gives a SF rate which is a 100 times smaller than the total rate near E_F. For fcc Co, we, furthermore, find that the structures in the directly computed SF probability and that obtained from Elliott's relation agree relatively well, however, Elliott's SF probability systematically overestimates the true SF probability by a factor four. This indicates that, depending on the studied material, the agreement between the two energy-resolved SF probabilities can range from being reasonable to poor, with Elliott's SF probability being typically larger by a factor of two to four.

B. Nonequilibrium hot electron spin lifetimes

The lifetimes as well as the spin lifetimes of excited nonthermal electrons due to electron-phonon scattering can be computed within our approach. To obtain these lifetimes at a given electron energy E above the Fermi energy, we define them as the average over all states having energy E. The average electron lifetimes correspond to the inverse scattering rate per number of states, i.e., $\tau_{\rm el}^{\sigma}(E) = n_\sigma(E)/\sum_{\sigma\sigma'} w_{\sigma\sigma'}(E)$, while the spin lifetimes are given as

$$\tau_{\rm SF}^{\sigma}(E) = n_\sigma(E)/w_{\uparrow\downarrow}(E)\,. \tag{19}$$

We assume that all other states above E_F are available for the NEQ electron to scatter into.

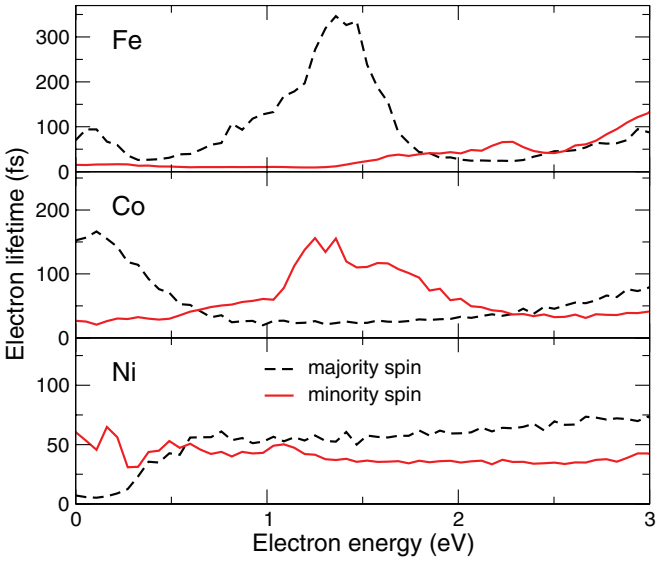

FIG. 7. (Color online) *Ab initio* computed spin-resolved electron lifetimes $\tau_{\rm el}^{\sigma}(E)$ caused by electron-phonon scattering of hot electrons in Fe, Co, and Ni, given as a function of the hot electron energy relative to the Fermi level at 0 eV.

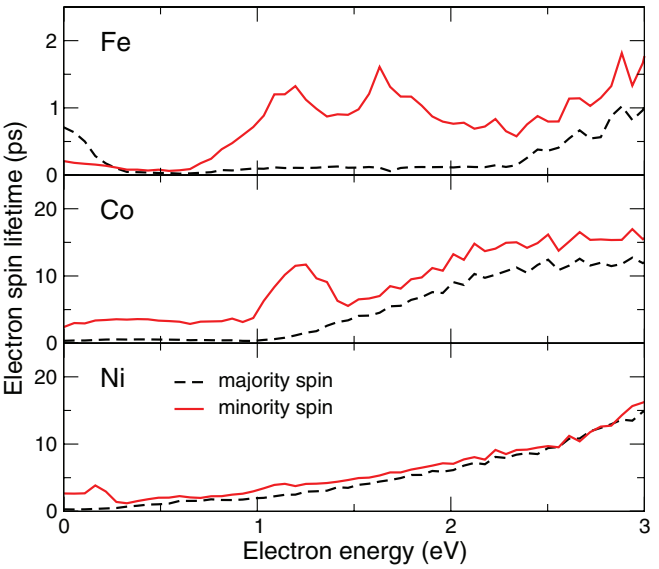

FIG. 8. (Color online) Computed spin-flip lifetimes $\tau_{\rm SF}^{\sigma}(E)$ of spin-polarized hot electrons due to electron-phonon scattering in Fe, Co, and Ni, given as a function of the electron energy relative to the Fermi level at 0 eV.

The calculated spin-resolved lifetimes $\tau_{\rm el}^{\sigma}(E)$ of hot electrons due to (spin-conserving) electron-phonon scattering of Fe, Co, and Ni are shown in Fig. 7. In some cases, the calculated electron-phonon lifetimes are on a comparable time scale as those due to electron-electron scattering.[69] This is most evident for minority-spin electrons in Fe for energies less than 1.5 eV, where we find hot electron lifetimes of around 10 fs for electron-phonon scattering, while very similar values have been predicted for electron-electron scattering.[69] In this situation, both processes contribute almost equally, thus halving the effective total lifetime, while for majority electrons the contribution coming from electron-phonon scattering is small. This observation could contribute to explain the observed spin asymmetry of the hot-electron mean free path in Fe,[70] which does not follow the expectation based on *ab initio* computed[69] electron-electron lifetimes. We find that the electron-phonon lifetimes can be quite energy as well as spin dependent, in particular for Fe and Co. The electron-phonon induced lifetime $\tau_{\rm el}^{\sigma}$ of Fe has a huge *spin asymmetry* for electrons with energies in the interval 0.7 to 1.7 eV, i.e., in the range of energies that can be reached by laser excitation. This is related to the *spin-resolved* scattering rates (not shown here). The strong energy dependence of the spin-resolved lifetimes occurs at energies where the d character of the bands prevails. At higher energies, where the hot electrons have mainly sp character, the electron-phonon lifetimes of majority- and minority-spin electrons are relatively comparable, having spin-averaged values of about 50 fs in Co and Ni, and up to 100 fs in Fe.

In Fig. 8, we show the *ab initio* computed electron-phonon induced electron spin lifetimes $\tau_{\rm SF}^{\sigma}(E)$ for all three $3d$ ferromagnets as a function of the nonthermal electron energy. A notable and common feature is the increase for higher energies, which is due to the s and p characters of these states becoming increasingly prominent. Simultaneously, the degree of spin mixing in these sp states is lower and the SF scattering rate therefore decreases. A further interesting feature is that for bcc Fe the order of the spin-majority and -minority lifetimes reverses below about 0.5 eV. A crossing of the Fe spin-majority and spin-minority lifetimes due to electron-electron scattering has been previously predicted below 1 eV.[69] The origin of this crossing has already been explained by phase space considerations, i.e., the amount of spin-majority and -minority phase spaces available for scatterings.[69] The hot electron spin lifetime in Fe is considerably smaller than that in Co and in Ni. This is due to the much larger scattering rate in Fe at 1–2 eV electron energy, see Fig. 4. The overall shape of the spin lifetimes also reflects the character of the unoccupied states. In Fe, there are unoccupied spin-majority d states up to about 0.5 eV, whereas there are spin-minority d states to about 2.5 eV. These states are responsible for the more pronounced structures below these energies. Above these energies, there are dominantly sp states giving relatively flat, slowly increasing spin lifetimes. In Ni, there are only spin-majority sp states present above E_F and the spin-minority d band extends to 0.3 eV, concomitant with the energy dependencies of the spin lifetimes seen in Fig. 8. Co adopts a position intermediate between Fe and Ni.

C. Electron-phonon generated demagnetization rates

1. Choice of hot electron distribution functions

We now turn to the demagnetizing influence of phonon-mediated SF scattering, particularly considering laser-heated ferromagnets. The determining quantities are the spin-resolved transition rates (11) and the demagnetization ratio D_S (14). The spin-resolved transition rates depend strongly on the spin-dependent electron distributions in the system. If $f_{\uparrow}(E) = f_{\downarrow}(E)$, the spin-increasing and spin-decreasing scattering rates S^{+} and S^{-} would be identical, and consequently, there would be no change of the total moment regardless of the value of the total SF probability, P_S. It is the imbalance between the scattering rates S^{+} and S^{-}, which is essential

for changing the moment [compare the two expressions in Eq. (12)]. The condition of unequal spin distributions is provided in ferromagnets with exchange-split spin-polarized bands, because the pump laser excitations will be different for the available spin-majority and -minority bands, which leads to generation of unequal spin populations. The laser excitation in itself is, to a good approximation, spin conserving, even in a full Dirac treatment with spin-orbit interaction.[71] The occurring spin (and charge) conservation can be imposed on the distributions by requiring

$$\int dE f_\sigma(E) n_\sigma(E) = \int dE f^0_\sigma(E) n_\sigma(E), \qquad (20)$$

where f^0_σ is the low-temperature Fermi-Dirac distribution.

Immediately following irradiation with the pump laser, the initial electron population is in a nonthermal state far from any Fermi-Dirac distribution. The excited hot electrons in this state thermalize by electron-electron scatterings, a process that leads within approximately 300 fs to a thermalized electron distribution.[72–76] The thermalized electron distributions are captured by Fermi-Dirac distributions with a high, spin-dependent electron temperature T_σ. As mentioned earlier, these hot, thermalized electrons are not yet in equilibrium with the lattice,[57] therefore we assume the phonons to be those of the equilibrium system. We further note that any spin relaxation occurring during electron-electron scattering is not treated here and has been studied elsewhere.[25,77]

The nonthermal[52] and thermalized electron distributions are computed here for similar total absorbed laser energies. The Fermi-Dirac distribution in the thermalized situation is given by a $f_\sigma(E) = f_{FD}(E, T_\sigma, \mu_\sigma)$; on account of the laser imparted energies electron temperatures of the order of a few thousands degrees of Kelvin can be expected. At such temperatures, the spin-dependent chemical potentials μ_σ are shifted from their equilibrium value and have to be determined by solving Eq. (20) numerically. Note that the shift in μ_σ has to go beyond the Sommerfeld expansion because the density of states changes significantly within the energy range set by the high electron temperature (3000 K corresponds to 0.26 eV).

The electron distributions present before thermalization are more difficult to describe. In principle, a nonmonotonic band, spin, and time-dependent occupation function $f_{b,\sigma}(E,t)$ would be needed, but such a precise description has not yet been achieved for real materials. Here, we therefore concentrate on its main features, which can be obtained from an optical conductivity calculation to simulate the influence of the pump laser. The influence of the pump laser on the total number of valence electrons is still relatively small, therefore the induced distribution can be given as an equilibrium distribution plus a deviation,[21,58] when assuming the usual fluences, which also implies that we do not have to consider any change in the band structure. The energy boundaries of the deviation are set by the frequency of the laser, inside this energy window the distribution is assumed to be flat. The critical component for magnetization dynamics is the spin-dependence of this distribution, see Eq. (12), therefore we concentrate on this feature.

The laser-created NEQ distributions are determined as follows. From $f_{\rm exc}$ excited electrons, $\gamma_\uparrow f_{\rm exc}$ are spin-up and $\gamma_\downarrow f_{\rm exc}$ are spin-down electrons, where $\gamma_\uparrow + \gamma_\downarrow = 1$. The ratio between excited spin majority and minority electrons $\gamma_\uparrow/\gamma_\downarrow$ is obtained from the *ab initio* calculated spin-resolved optical conductivity Re $[\sigma_{xx}(\omega)]$,[21,78] where the exciting laser frequency $\omega = 1.55$ eV is assumed. The quantities related to the regions $[E_F - \hbar\omega, E_F]$ and $[E_F, E_F + \hbar\omega]$ are marked with superscripts $<$ and $>$, respectively. Employing the total numbers of spin majority and minority electrons in these regions, $N^<_\sigma$ and $N^>_\sigma$, one obtains the spin-dependent occupation factors relative to $f_{\rm exc}$: $f^<_\sigma = (\gamma_\sigma/N^<_\sigma) f_{\rm exc}$ and equivalently for $f^<_\sigma$. The *ab initio* computed numbers for Ni, Fe, and Co are given in Table I.

TABLE I. Given are the spin-decomposition of the optical transitions γ_σ induced by an $\omega = 1.55$ eV laser, number of electrons $N^<_\sigma$ and $N^>_\sigma$ accommodated in the energy windows $[E_F - \hbar\omega, E_F]$ and $[E_F, E_F + \hbar\omega]$ as well as their resulting occupations $f^<_\sigma$ and $f^>_\sigma$.

atom, σ	γ_σ	$N^<_\sigma$	$f^<_\sigma/f_{\rm exc}$	$N^>_\sigma$	$f^>_\sigma/f_{\rm exc}$
Ni ↑	36%	1.65	0.22	0.22	1.65
Ni ↓	64%	1.38	0.46	0.69	0.92
Fe ↑	29%	2.11	0.14	0.35	0.83
Fe ↓	71%	1.43	0.50	1.34	0.53
Co ↑	28%	1.62	0.17	0.24	1.19
Co ↓	72%	1.66	0.44	1.67	0.43

This significantly limits SF contributions from the high binding energy region, where a high number of spin-flips take place in the case of nonthermal electron distributions. Furthermore, the largest imbalance between minority and majority occupation numbers appears at energies above E_F.[46]

2. *Computed results*

The main results of the electron-phonon induced SF scattering are collected in Table II. To start with, the Elliott SF probabilities $P^{b^2}_S$ computed in this work are compared with previously computed Elliott probabilities of Steiauf and Fähnle,[44] as well as with the exact electron-phonon SF probabilities P_S. Our calculated Elliott probabilities are comparable

TABLE II. Given are *ab initio* calculated spin-flip probabilities P_S, Elliott SF probability $P^{b^2}_S$, demagnetization ratios D_S, and relative demagnetization fractions $\Delta M/M_0$ for laser-pumped Ni, Fe, and Co. Calculated values are given for equilibrium (low T), for thermalized electrons at a high Fermi temperature T_e, and for the nonequilibrium (NEQ) electron distribution created by femtosecond laser excitation. Computed values for the approximate Elliott SF probability $P^{b^2}_S$ are compared to values from Ref. 44. The relative demagnetization fraction $\Delta M/M_0$, achieved by electron-phonon SF scattering, is given in % at 250 fs.

	$P^{b^2}_S$	P_S	D_S	$\Delta M/M_0$
Ni (low T)	0.07 (0.10[44])	0.04	0	0
Ni ($T_e = 3000$ K)	0.11	0.07	0.003	3.1
Ni (NEQ)	0.12	0.09	0.025	16.7
Fe (low T)	0.068 (0.096[44])	0.04	0	0
Fe ($T_e = 3000$ K)	0.13	0.09	0.008	4.5
Fe (NEQ)	0.14	0.07	0.030	11.4
Co (low T)	0.060 (0.044[44])	0.010	0	0
Co ($T_e = 3000$ K)	0.095	0.017	0.002	0.9
Co (NEQ)	0.105	0.022	0.010	2.3

(∼30%) with the earlier computed ones; a somewhat larger deviation of 36% is present for fcc Co.[44] The deviation between the Elliott SF probability $P_S^{b^2}$ and the true SF probability is notably larger, ranging from a factor of two to six. The deviation is particularly large for fcc Co. Contrary to previous results (based on the Elliott approximation)[44] for Co, we predict a SF probability P_S of Co that is four times lower than that of Ni, also in the excited regime.

Steiauf and Fähnle[44] have estimated the Elliott probability $P_S^{b^2}$ (denoted as α_{sf} in Ref. 15) for the laser-excited ferromagnets Ni and Co by averaging the energy-dependent spin-mixing probability $\langle b^2(E)\rangle$ using a Gaussian with standard deviation $\sigma = 1.4$ eV around E_F. They obtained thereby enhanced probabilities $\alpha_{sf} = P_S^{b^2}$ of 0.18 and 0.196 for Ni and Co, respectively. These values cannot be directly compared to our computed values for the laser-irradiated materials in Table II as there we have used explicitly NEQ and thermalized electron distributions to simulate the effect of the pump laser. It may be noted, however, that the difference with the exact SF probability P_S can be large, up to a factor of 10 for Co.

Considering next the electron-phonon SF probabilities P_S in comparison with the demagnetization ratios D_S, we observe that the latter are substantially smaller than the former. For a laser-heated thermalized electron gas, the demagnetization ratios D_S are about ten times smaller than P_S, exemplifying that there can be a moderately high total SF probability, which, however, with nearly as many spin-increasing as spin-decreasing SF events does not give rise to an appreciable demagnetization.

As noted previously[46] for fcc Ni, a somewhat larger SF probability but a drastically larger demagnetization ratio is obtained for the highly NEQ state immediately after laser excitation. This is observed for all three ferromagnets. The mechanism of the larger NEQ demagnetization ratio is complex as it involves hole and electron contributions, above and below E_F. To understand the significantly weaker demagnetization ratio in the thermalized regime, one may note that in all studied metals the highest SF rates were found to be positioned at least 0.5 eV below the Fermi level. However, in the electron thermalized situation for the here-studied temperatures the difference between the Fermi-Dirac distributions at high-temperature and at zero temperature becomes small for energies of more than 0.5 eV below E_F (difference becomes less than 0.1 for 3000 K). This significantly limits SF contributions from the higher binding-energy region, where a high number of spin-flips takes place in the case of nonthermal electron distributions. In addition, the largest imbalance between minority and majority occupation numbers appears, for all three ferromagnets in the electron thermalized situation, at energies above E_F.[46] Hence, we observe that SF electron-phonon scattering is efficient only as long as the electron spin-distributions are in a highly NEQ state, with significant contributions coming from deep-lying hole states.

The calculated electron-phonon mediated relative demagnetization fractions $\Delta M/M_0$, which are a central outcome of our investigation, are given in Table II. ΔM denotes $M_0 - M(\tau)$, and M_0 is the computed static equilibrium moment; the values for M_0 are 2.2, 1.6, and 0.64μ_B for Fe, Co, and Ni. The resulting demagnetization fractions $\Delta M/M_0$ are expressed in percentage of demagnetization at time $\tau = 250$ fs. The time interval of 250 fs is chosen for the following reasons: laser-induced demagnetization experiments show that the process of demagnetization is completed at about 250 fs in ferromagnetic transition metals[24,50,79,80] and their alloys.[49] The computed relative demagnetizations can thus directly be compared with experimental data. Furthermore, photoemission experiments on the evolution of the laser-induced NEQ state show that this state evolves into an electron thermalized state within about the same time.[72,74–76] Once the NEQ state has thermalized the large contribution to the SF ratio has vanished. As it is not precisely known how the nonthermal state evolves to a thermalized one, we assume here for simplicity that the NEQ state decays linearly with time to a thermalized state in 250 fs. Conversely, for the calculations of $\Delta M/M_0$ in the electron thermalized state, we assume that this state is stable over 250 fs, i.e., it is assumed that the electron thermalized state is formed instantaneously upon laser excitation and then persists. This is an approximation, as there will be a transfer of energy from the hot electrons to the lattice. However, recent measurements showed that it takes about 3 ps for the lattice to heat up;[57] hence, its influence is estimated to be limited within 250 fs.

The calculated relative demagnetization fractions due to electron-phonon SF scattering are negligible at low temperatures, as could be expected. A more important outcome of our calculations is that at relatively high electron temperatures of 3000 K the achieved amount of demagnetization is only a few percent. In particular, the rather small computed values show that phonon-mediated SF scattering in the thermalized situation cannot explain the experimentally observed demagnetizations of the order of 50%.[1,15,50,81,82] Alternatively, using $dM(t)/dt|_{t=0} = -[M_0 - M_{\text{min.}}]/\tau_M$ we can estimate the time τ_M needed to achieve a 50% demagnetization, $M_{\text{min.}} = 0.5M_0$. For an electron temperature of 3000 K this gives 3, 14, and 4 ps, respectively, for Fe, Co, and Ni. These demagnetization times computed for the electron-thermalized regime are considerably longer than the experimental ones.

The situation is quite different for NEQ electron distributions. These can give an appreciable contribution to the total demagnetization; notably, the resulting values are strongly material dependent. A moderately high relative demagnetization of 17% is computed for Ni, whereas for Co it is only 2%. These surprising materials' dependencies are directly born out of the energy-resolved electron-phonon SF scattering rates, which markedly depend on the spin-polarized electronic structures near E_F. Irrespective, the total computed electron-phonon mediated demagnetizations do not reach the experimental demagnetizations of about 50%.

The surprising materials dependencies can be explained in terms energy-dependent SF scattering rates and the particular shapes of the spin-polarized DOS in each of the ferromagnets, but an extensive analysis is outside of the focus of the present study. We briefly mention that, due to the d-band positions, the SF scattering rate in the region $E > E_F$ is very low for Ni, but much larger for Fe. The demagnetization in the thermalized regime is therefore relatively small and only weakly temperature dependent in Ni, but in Fe, it is not suppressed as strongly. In Fe, the peak in the SF scattering rate above E_F (see Fig. 4) contributes to the effective demagnetization rate through spin-decreasing transitions in the electron channel.

This leads to the highest computed demagnetization gradient $dM/dt(t=0)$ of the studied materials, being counterbalanced by the highest static moment M_0.

IV. DISCUSSION

A paramount outcome of our *ab initio* investigation is that electron-phonon SF scattering processes in the electron thermalized regime cannot account for observed laser-induced demagnetizations. Before this can be definitely established, it is, however, required, first, to critically discuss the approximations in our approach, and second, compare with other recent calculations.

Recently, Essert and Schneider[47] performed an *ab initio* investigation in which they carried out a direct electron-phonon matrix calculation, employing the rigid-ion approximation, to compute SF probabilities in fcc Ni and bcc Fe. They, furthermore, calculated the demagnetization rate employing the Boltzmann equation. The computed thermalized demagnetization fractions are of the order of a few percent, in good agreement with our values. This is furthermore consistent with our findings, which show that Eliashberg functions computed with the rigid-ion approximation agree quite well with Eliashberg functions computed without such approximation (see Fig. 1).

Estimations of the effectiveness of the electron-phonon Elliott-Yafet SF contribution in the laser-induced demagnetization were made recently,[15,45] employing the microscopic three-temperature model (M3TM)[15,83] as well as computed Elliott SF probabilities, $P_S^{b^2}$. The main conclusion drawn in these investigations was that the electron-phonon SF scattering in the electron thermalized regime can very well account for the measured demagnetizations and that the influence of highly excited electronic states can be disregarded. Remarkably, our *ab initio* investigations lead to precisely opposite conclusions—the effective demagnetization reached in a thermalized electron system is quite small (∼3%), but appreciably larger values result from NEQ excited distributions. Hence an important question to be addressed is why the M3TM predicts much larger phonon-mediated demagnetization values than *ab initio* based calculations, which will be done further below.

Discussing now the approximations made in our approach, we start with noting that it is essential to distinguish between transversal and longitudinal magnetization relaxations. Transversal spin excitations are important for the relatively slow magnetization precession on the pico- to nanosecond scale, whereas longitudinal spin excitations might provide a channel for subpicosecond demagnetization. We have excluded the transversal spin excitations in our calculations since they are not a part of the common definition of Elliott-Yafet SF scattering.[59]

First, *a priori* it is not evident if our starting point, the Kohn-Sham LSDA band structure, nominally valid at $T=0$, is sufficient to describe spin excitations in the $3d$ ferromagnets. It has been argued[84] that such a "rigid" band structure cannot be used to describe demagnetization due to spin excitations. It may be noted that it has been shown[85,86] previously that such zero-temperature band structure can very well be employed to accurately compute the transversal spin-excitation energy spectra of Fe, Co, and Ni, as well as their temperature-dependent magnetization $M(T)$. However, as prior to our calculations, no *ab initio* calculations of the longitudinal Elliott-Yafet electron-phonon spin-flip spectrum existed (to the best of our knowledge), we can presently not state how accurate such calculations are, but we may note (1) that our calculation for Al is in good agreement with an earlier work[56] and (2) the recently published independent computational investigation[47] obtained very similar demagnetization fractions in the thermalized regime.

Second, our calculations pertain to demagnetization effects in the linear regime, i.e., at times immediately after the action of the laser pulse when the demagnetization sets in. We do not study a complete time evolution, but we obtain the magnetization's time derivative at $t=0$, $dM(t)/dt|_{t=0} = -[M(0)-M_{\min}]/\tau_M$, giving the demagnetization rate. This is consistent with the commonly-used fit function $M(t)-M(0) \approx -[M(0)-M_{\min}](1-e^{-t/\tau_M})$ (note that the remagnetization happening on much longer times is neglected here). A consequence of the here-assumed linear regime is that it does not take the effect of already occurred spin-flips on the spin-polarized band structure into account. It could be that the demagnetization might accelerate cumulatively with the number of SF scattering events.[45] If this would be the case, the time-dependent magnetization $M(t)$ would be a concave function. However, $M(t)$ is always observed to be a convex function in experiments and simulations. Thus, extrapolating $M(t)$ from its linear behavior at $t=0$, we would always be only overestimating the effective demagnetization. Furthermore, the peak achieved demagnetization has been observed experimentally to depend linearly on the fluence in a broad range of fluences,[45,81] which further justifies using the linear regime and the neglect of second-order effects like that of already occurred spin flips.

Third, it has been recently argued[45,84,87] that in order to achieve a sizable ultrafast demagnetization one would need to take into account an additional mechanism, besides the Elliott-Yafet electron-phonon SF scatterings, for instance, an ultrafast dynamical reduction of the exchange splitting. As mentioned above, through already occurred SF events the exchange splitting would be somewhat reduced, however, this reduction is quite small initially, and it happens on time scales that are relatively long compared to that observed for femtosecond demagnetization. Moreover, as the origin of exchange splitting is the Pauli exclusion principle, it is not clear how an ultrafast dynamic reduction can be achieved.

Fourth, we note that the spin-flip processes studied in our model require significantly lower energy than Stoner excitations, because the SF scattering changes the electron energy only negligibly. The spin-flipped electron enters an empty state (hole) left by another previously laser-excited electron, or alternatively the spin-flipped hot electron had already acquired a high energy before undergoing a spin flip. The necessary energy has thus already been gained from the pump laser and, in contrast to Stoner excitations, it is not needed for enabling the spin flip.

Next, in order to understand why our conclusions regarding the efficiency of the Elliott-Yafet SF mechanism are so different from recent evaluations on the basis of the M3TM model,[15] we analyze more thoroughly the assumptions underlying the M3TM. In the M3TM, there is a disputable

separation of electronic and spin degrees of freedom adopted;[83] the equilibration of the spin system with the lattice is driving the demagnetization. Further, the sharply peaked structures of the spin-polarized DOS, typical for each of the transition metals, have been assumed to be constant. The difference between our computed exact SF probabilities P_S and the Elliott SF probabilities $P_S^{b^2}$ used[15] in the M3TM is a factor of 2 for Ni, which may not be as significant as to lead to opposite conclusions, but it is a factor 10 for Co. The crucial quantity that we identified for an ultrafast demagnetization[46] is the imbalance between spin-increasing and spin-decreasing spin flips, which correspond directly to the demagnetization rate. The essential difference between the M3TM and our calculations appears when this quantity is computed, in the second step of the calculation to obtain dM/dt. Taking a closer look at how this imbalance is provided in the M3TM, we note that the spin change rate dS/dt is expressed as SF probability a_{sf} multiplied with transition factors that contain, e.g., $[1 - f(E)]f(E + \Delta_{\text{ex}} + E_{\text{ph}})$, where f is the Fermi function at an electron temperature T_e, Δ_{ex} the exchange splitting, and E and E_{ph} are the electron and phonon energies, respectively [see Eqs. (5.10) and (5.20) in Ref. 83]. The assumption behind this is that when a spin is flipped in the M3TM (in which electron and spin systems are separated) the spin system gains energy Δ_{ex} and the electron system looses energy Δ_{ex}, see Fig. 5.2 of Ref. 83. The spin-flipped electron is thus assumed to have a changed energy, e.g., $E + \Delta_{\text{ex}} + E_{\text{ph}}$, which is inserted in the Fermi-Dirac distribution. In our calculations, we used instead transition factors $[1 - f_\sigma(E)]\ f_{\sigma'}(E + \hbar\Omega)$, see Eq. (7), which express that when an electron scatters from one state to another, the two states can have energies different up to the phonon energy $\hbar\Omega$ $(=E_{\text{ph}})$. The M3TM conversely assumes that the electron scatters with a phonon to a spin-reversed state having a very large energy difference $\pm\Delta_{\text{ex}} \pm E_{\text{ph}}$ together with an energy gain $\mp\Delta_{\text{ex}}$ of the spin system. We note that, as the exchange splitting Δ_{ex} ($\approx$1–2 eV) is much larger than the typical phonon energy ($\sim$30 meV), it is not very probable that an electron can change its energy by Δ_{ex} in the electron-phonon scattering process. Employing such a massively changed electron energy in products of the form $[1 - f(E)]f(E + \Delta_{\text{ex}} + E_{\text{ph}})$ will lead to spin-dependent transition rates that are vastly bigger than those obtained with $[1 - f(E)]f(E + \hbar\Omega) \approx [1 - f(E)]f(E)$, as done in our approach. Consequently, because of the assumption made in the M3TM model, the transition factors are overestimated. This explains the difference of results between our model and M3TM (up to a factor of 50). Nonetheless, drawing a final conclusion about the demagnetization mechanism is still not possible at this stage, because there are several effects not present neither in the M3TM not in our model (for example, possible modification of band structure, exchange splitting and exchange constants due to the pump pulse), and in addition, the electron redistribution following the pulse is not accurately described in both models.

V. CONCLUSIONS

We have developed a theoretical treatment on the basis of a generalized spin- and energy- dependent Eliashberg function to investigate computationally the Elliott-Yafet electron-phonon mediated ultrafast spin relaxation in ferromagnetic transition metals. The formalism has been used—in combination with full-potential relativistic electronic structure calculations as well as *ab initio* computed phonon dispersions—to obtain materials' specific, quantitative information with respect to the extent of ultrafast demagnetization that can be caused by spin-flip processes generated by electron-phonon scatterings in the 3*d* transition metals Fe, Co, and Ni. Our investigations specifically aim at clarifying the possible contribution of Elliott-Yafet phonon-mediated spin-flip scatterings to the experimentally observed laser-induced ultrafast demagnetization. As yet, these processes are still poorly understood, especially on the *ab initio* level. Our calculations reveal interesting and unexpected differences in the spin-relaxation behaviors of the three materials. The calculated electron-phonon SF probability is observed to be strongly dependent on the electron single-particle energy. Also, the computed energy- and spin-dependent hot electron and spin lifetimes exhibit considerable, unanticipated, differences for the three 3*d* ferromagnets. The electron lifetime of a hot electron in Fe has, for example, a much larger spin asymmetry than a hot electron in Ni.

As it has been proposed[15] that electron-phonon spin-flip scatterings in the electron thermalized regime could well account for the observed femtosecond demagnetization, we have computed the electron-phonon mediated demagnetization rate both for laser-created thermalized electron distributions as well as nonequilibrium (i.e., nonthermal) electron distributions. Our calculations aim at acquiring a more detailed understanding of the possible contribution of Elliott-Yafet processes to the ultrafast demagnetization. We have found that generally a difference of SF probabilities in states above and below Fermi level are important. Taking this energy dependence of the *ab initio* SF probabilities into account, we find that Elliott-Yafet SF processes in the electron thermalized regime cannot account for the experimentally observed ultrafast demagnetization. Interestingly, the Elliott-Yafet phonon-mediatied mechanism is computed to be much more efficient (by a factor of 3 to 5) for nonthermal laser-created electron distributions, as these enhance the imbalance of spin increasing and spin decreasing SF scatterings. Hence, we can conclude that the dominant contribution of the Elliott-Yafet mechanism to ultrafast demagnetization has a nonthermal character and is expected to occur in the first few hundred femtoseconds, immediately after laser excitation. The largest nonthermal Elliott-Yafet phonon-mediated demagnetization is computed for fcc Ni where it can reach about 17% at 250 fs. While this is not negligible, it is not sufficient to explain the measured[1,50,81,82] laser-induced demagnetizations of 50% or more. Summarizing, our calculations suggest that Elliott-Yafet electron-phonon SF scattering alone cannot account for the observed ultrafast laser-induced demagnetizations; a different mechanism may be dominant here. Recent experiments[30–32] suggest fast, nonequilibrium transport of spin-polarized hot carriers as a plausible source.

Lastly, we have compared our results with those previously obtained with the M3TM model. A significant difference between our approach and the M3TM model lies in the way the demagnetization rate is assigned with a given SF probability.

As outlined above, we believe that this is done in a more accurate way in our theory than in the M3TM model.

ACKNOWLEDGMENTS

We acknowledge Christian Schneider, Sven Essert, and Manfred Fähnle for useful discussions. This work has been supported by the Swedish Research Council (VR), the G. Gustafsson Foundation, the Czech Science Foundation (P204/11/P481), and the European Community's Seventh Framework Programme (FP7/2007-2013) under grant agreements Nos. 214810 "FANTOMAS" and 281043 "FemtoSpin." Support through the Swedish National Infrastructure for Computing (SNIC) is gratefully acknowledged. The National Center CERIT Scientific Cloud (CERIT-SC) of the Czech Republic is acknowledged for providing the computer facilities to support part of the present calculations under Grant Reg. No. CZ.1.05/3.2.00/08.0144. D. Legut acknowledges a support within the framework of the Nanotechnology Centre (the basis for international cooperation project), Reg. No. CZ.1.07/2.3.00/20.0074 and the IT4Innovations Centre of Excellence project, Reg. No. CZ.1.05/1.1.00/02.0070, both supported by the Operational Programme "Education for competitiveness" funded by Structural Funds of the European Union and state budget of the Czech Republic.

*karel.carva@fysik.uu.se

[1] E. Beaurepaire, J.-C. Merle, A. Daunois, and J.-Y. Bigot, Phys. Rev. Lett. **76**, 4250 (1996).
[2] A. V. Kimel, A. Kirilyuk, P. A. Usachev, R. V. Pisarev, A. M. Balbashov, and T. Rasing, Nature (London) **435**, 655 (2005).
[3] A. Kirilyuk, A. V. Kimel, and T. Rasing, Rev. Mod. Phys. **82**, 2731 (2010).
[4] J.-Y. Bigot, M. Vomir, and E. Beaurepaire, Nat. Phys. **5**, 515 (2009).
[5] I. Tudosa, C. Stamm, A. B. Kashuba, F. King, H. C. Siegmann, J. Stohr, G. Ju, B. Lu, and D. Weller, Nature (London) **428**, 831 (2004).
[6] J. Hohlfeld, E. Matthias, R. Knorren, and K. H. Bennemann, Phys. Rev. Lett. **78**, 4861 (1997).
[7] G. Ju, A. Vertikov, A. V. Nurmikko, C. Canady, G. Xiao, R. F. C. Farrow, and A. Cebollada, Phys. Rev. B **57**, R700 (1998).
[8] H. Regensburger, R. Vollmer, and J. Kirschner, Phys. Rev. B **61**, 14716 (2000).
[9] K. Vahaplar, A. M. Kalashnikova, A. V. Kimel, D. Hinzke, U. Nowak, R. Chantrell, A. Tsukamoto, A. Itoh, A. Kirilyuk, and T. Rasing, Phys. Rev. Lett. **103**, 117201 (2009).
[10] I. Radu, K. Vahaplar, C. Stamm, T. Kachel, N. Pontius, H. A. Durr, T. A. Ostler, J. Barker, R. F. L. Evans, R. W. Chantrell, A. Tsukamoto, A. Itoh, A. Kirilyuk, T. Rasing, and A. V. Kimel, Nature (London) **472**, 205 (2011).
[11] T. A. Ostler, J. Barker, R. F. L. Evans, R. W. Chantrell, U. Atxitia, O. Chubykalo-Fesenko, S. El Moussaoui, L. Le Guyader, E. Mengotti, L. J. Heyderman, F. Nolting, A. Tsukamoto, A. Itoh, D. Afanasiev, B. A. Ivanov, A. M. Kalashnikova, K. Vahaplar, J. Mentink, A. Kirilyuk, T. Rasing, and A. V. Kimel, Nat. Commun. **3**, 666 (2012).
[12] U. Bovensiepen, Nat. Phys. **5**, 461 (2009).
[13] G. M. Müller, J. Walowski, M. Djordjevic, G.-X. Miao, A. Gupta, A. V. Ramos, K. Gehrke, V. Moshnyaga, K. Samwer, J. Schmalhorst, A. Thomas, A. Hutten, G. Reiss, J. S. Moodera, and M. Münzenberg, Nat. Mater. **8**, 56 (2009).
[14] G. P. Zhang, W. Hubner, G. Lefkidis, Y. Bai, and T. F. George, Nat. Phys. **5**, 499 (2009).
[15] B. Koopmans, G. Malinowski, F. Dalla Longa, D. Steiauf, M. Fähnle, T. Roth, M. Cinchetti, and M. Aeschlimann, Nat. Mater. **9**, 259 (2010).
[16] K. Carva, M. Battiato, and P. M. Oppeneer, Nat. Phys. **7**, 665 (2011).
[17] G. P. Zhang and W. Hübner, Phys. Rev. Lett. **85**, 3025 (2000).
[18] B. Koopmans, M. van Kampen, and W. J. M. de Jong, J. Phys.: Condens. Matter **15**, S723 (2003).
[19] B. Koopmans, M. van Kampen, J. T. Kohlhepp, and W. J. M. de Jonge, Phys. Rev. Lett. **85**, 844 (2000).
[20] T. Kampfrath, R. G. Ulbrich, F. Leuenberger, M. Münzenberg, B. Sass, and W. Felsch, Phys. Rev. B **65**, 104429 (2002).
[21] P. M. Oppeneer and A. Liebsch, J. Phys.: Condens. Matter **16**, 5519 (2004).
[22] L. Guidoni, E. Beaurepaire, and J.-Y. Bigot, Phys. Rev. Lett. **89**, 017401 (2002).
[23] B. Koopmans, H. H. J. E. Kicken, M. van Kampen, and W. J. M. de Jonge, J. Magn. Magn. Mater. **286**, 271 (2005).
[24] E. Carpene, E. Mancini, C. Dallera, M. Brenna, E. Puppin, and S. De Silvestri, Phys. Rev. B **78**, 174422 (2008).
[25] M. Krauss, T. Roth, S. Alebrand, D. Steil, M. Cinchetti, M. Aeschlimann, and H. C. Schneider, Phys. Rev. B **80**, 180407 (2009).
[26] A. B. Schmidt, M. Pickel, M. Donath, P. Buczek, A. Ernst, V. P. Zhukov, P. M. Echenique, L. M. Sandratskii, E. V. Chulkov, and M. Weinelt, Phys. Rev. Lett. **105**, 197401 (2010).
[27] M. Battiato, K. Carva, and P. M. Oppeneer, Phys. Rev. Lett. **105**, 027203 (2010).
[28] M. Battiato, K. Carva, and P. M. Oppeneer, Phys. Rev. B **86**, 024404 (2012).
[29] A. Melnikov, I. Razdolski, T. O. Wehling, E. T. Papaioannou, V. Roddatis, P. Fumagalli, O. Aktsipetrov, A. I. Lichtenstein, and U. Bovensiepen, Phys. Rev. Lett. **107**, 076601 (2011).
[30] D. Rudolf, C. La-O-Vorakiat, M. Battiato, R. Adam, J. M. Shaw, E. Turgut, P. Maldonado, S. Mathias, P. Grychtol, H. T. Nembach, T. J. Silva, M. Aeschlimann, H. C. Kapteyn, M. M. Murnane, C. M. Schneider, and P. M. Oppeneer, Nat. Commun. **3**, 1037 (2012); E. Turgut, C. La-o vorakiat, J. M. Shaw, P. Grychtol, H. T. Nembach, D. Rudolf, R. Adam, M. Aeschlimann, C. M. Schneider, T. J. Silva, M. M. Murnane, H. C. Kapteyn, and S. Mathias, Phys. Rev. Lett. **110**, 197201 (2013).
[31] B. Vodungbo, J. Gautier, G. Lambert, A. Barszczak-Sardinha, M. Lozano, S. Sebban, M. Ducousso, W. Boutu, K. Li, B. Tudu, M. Tortarolo, R. Hawaldar, R. Delaunay, V. López-Flores, J. Arabski, C. Boeglin, H. Merdji, P. Zeitoun, and J. Lüning, Nat. Commun. **3**, 999 (2012).
[32] B. Pfau, S. Schaffert, L. Müller, C. Gutt, A. Al-Shemmary, F. Büttner, R. Delaunay, S. Düsterer, S. Flewett, R. Frömter *et al.*, Nat. Commun. **3**, 1100 (2012).

[33]U. Atxitia, O. Chubykalo-Fesenko, N. Kazantseva, D. Hinzke, U. Nowak, and R. W. Chantrell, Appl. Phys. Lett. **91**, 232507 (2007).
[34]N. Kazantseva, D. Hinzke, U. Nowak, R. W. Chantrell, U. Atxitia, and O. Chubykalo-Fesenko, Phys. Rev. B **77**, 184428 (2008).
[35]U. Atxitia, O. Chubykalo-Fesenko, J. Walowski, A. Mann, and M. Münzenberg, Phys. Rev. B **81**, 174401 (2010).
[36]U. Atxitia and O. Chubykalo-Fesenko, Phys. Rev. B **84**, 144414 (2011).
[37]K. Vahaplar, A. M. Kalashnikova, A. V. Kimel, S. Gerlach, D. Hinzke, U. Nowak, R. Chantrell, A. Tsukamoto, A. Itoh, A. Kirilyuk, and T. Rasing, Phys. Rev. B **85**, 104402 (2012).
[38]J. H. Mentink, J. Hellsvik, D. V. Afanasiev, B. A. Ivanov, A. Kirilyuk, A. V. Kimel, O. Eriksson, M. I. Katsnelson, and T. Rasing, Phys. Rev. Lett. **108**, 057202 (2012).
[39]M. Sultan, U. Atxitia, A. Melnikov, O. Chubykalo-Fesenko, and U. Bovensiepen, Phys. Rev. B **85**, 184407 (2012).
[40]R. J. Elliott, Phys. Rev. **96**, 266 (1954).
[41]B. Koopmans, J. J. M. Ruigrok, F. D. Longa, and W. J. M. de Jonge, Phys. Rev. Lett. **95**, 267207 (2005).
[42]M. Fähnle, J. Seib, and C. Illg, Phys. Rev. B **82**, 144405 (2010).
[43]M. Fähnle and C. Illg, J. Phys.: Condens. Matter **23**, 493201 (2011).
[44]D. Steiauf and M. Fähnle, Phys. Rev. B **79**, 140401 (2009).
[45]T. Roth, A. J. Schellekens, S. Alebrand, O. Schmitt, D. Steil, B. Koopmans, M. Cinchetti, and M. Aeschlimann, Phys. Rev. X **2**, 021006 (2012).
[46]K. Carva, M. Battiato, and P. M. Oppeneer, Phys. Rev. Lett. **107**, 207201 (2011).
[47]S. Essert and H. C. Schneider, Phys. Rev. B **84**, 224405 (2011).
[48]C. La-O-Vorakiat, M. Siemens, M. M. Murnane, H. C. Kapteyn, S. Mathias, M. Aeschlimann, P. Grychtol, R. Adam, C. M. Schneider, J. M. Shaw, H. Nembach, and T. J. Silva, Phys. Rev. Lett. **103**, 257402 (2009).
[49]S. Mathias, C. La-O-Vorakiat, P. Grychtol, P. Granitzka, E. Turgut, J. M. Shaw, R. Adam, H. T. Nembach, M. E. Siemens, S. Eich, C. M. Schneider, T. J. Silva, M. Aeschlimann, M. M. Murnane, and H. C. Kapteyn, Proc. Natl. Acad. Sci. USA **109**, 4792 (2012).
[50]C. Stamm, T. Kachel, N. Pontius, R. Mitzner, T. Quast, K. Holldack, S. Khan, C. Lupulescu, E. F. Aziz, M. Wietstruk, H. A. Dürr, and W. Eberhardt, Nat. Mater. **6**, 740 (2007).
[51]M. Wietstruk, A. Melnikov, C. Stamm, T. Kachel, N. Pontius, M. Sultan, C. Gahl, M. Weinelt, H. A. Dürr, and U. Bovensiepen, Phys. Rev. Lett. **106**, 127401 (2011).
[52]K. Carva, D. Legut, and P. M. Oppeneer, Europhys. Lett. **86**, 57002 (2009).
[53]J. Fabian and S. Das Sarma, Phys. Rev. Lett. **81**, 5624 (1998).
[54]G. Grimvall, *Electron-Phonon Interaction in Metals*, edited by E. P. Wohlfarth (North-Holland, Amsterdam, 1981).
[55]P. K. Lam, M. M. Dacorogna, and M. L. Cohen, Phys. Rev. B **34**, 5065 (1986).
[56]J. Fabian and S. Das Sarma, Phys. Rev. Lett. **83**, 1211 (1999).
[57]X. Wang, S. Nie, J. Li, R. Clinite, J. E. Clark, and J. Cao, Phys. Rev. B **81**, 220301 (2010).
[58]J. Hohlfeld, S. S. Wellershoff, J. Güdde, U. Conrad, V. Jähnke, and E. Matthias, Chem. Phys. **251**, 237 (2000).
[59]Y. Yafet, in *Solid State Physics*, edited by F. Seitz and D. Turnbull, Vol. 14 (Academic, New York, 1963), Chap. 2, p. 59.
[60]L. M. Sandratskii and P. Mavropoulos, Phys. Rev. B **83**, 174408 (2011).
[61]A. W. Overhauser, Phys. Rev. **89**, 689 (1953).
[62]F. Beuneu and P. Monod, Phys. Rev. B **18**, 2422 (1978).
[63]W. Kohn and L. J. Sham, Phys. Rev. **140**, A1133 (1965).
[64]J. P. Perdew and Y. Wang, Phys. Rev. B **45**, 13244 (1992).
[65]A. Dal Corso and S. de Gironcoli, Phys. Rev. B **62**, 273 (2000).
[66]L. Nordheim, Ann. Phys. **401**, 607 (1931).
[67]X. Y. Wang, D. M. Riffe, Y.-S. Lee, and M. C. Downer, Phys. Rev. B **50**, 8016 (1994).
[68]Z. Lin, L. V. Zhigilei, and V. Celli, Phys. Rev. B **77**, 075133 (2008).
[69]V. P. Zhukov, E. V. Chulkov, and P. M. Echenique, Phys. Rev. B **73**, 125105 (2006).
[70]T. Banerjee, J. C. Lodder, and R. Jansen, Phys. Rev. B **76**, 140407 (2007).
[71]T. Kraft, P. M. Oppeneer, V. N. Antonov, and H. Eschrig, Phys. Rev. B **52**, 3561 (1995).
[72]C.-K. Sun, F. Vallée, L. Acioli, E. P. Ippen, and J. G. Fujimoto, Phys. Rev. B **48**, 12365 (1993).
[73]N. Del Fatti, C. Voisin, M. Achermann, S. Tzortzakis, D. Christofilos, and F. Vallée, Phys. Rev. B **61**, 16956 (2000).
[74]C. Guo, G. Rodriguez, and A. J. Taylor, Phys. Rev. Lett. **86**, 1638 (2001).
[75]H.-S. Rhie, H. A. Dürr, and W. Eberhardt, Phys. Rev. Lett. **90**, 247201 (2003).
[76]M. Lisowski, P. A. Loukakos, U. Bovensiepen, J. Stähler, C. Gahl, and M. Wolf, Appl. Phys. A **78**, 165 (2004).
[77]V. P. Zhukov, E. V. Chulkov, and P. M. Echenique, Phys. Status Solidi A **205**, 1296 (2008).
[78]K. Hild, G. Schönhense, H. J. Elmers, T. Nakagawa, T. Yokoyama, K. Tarafder, and P. M. Oppeneer, Phys. Rev. B **85**, 014426 (2012).
[79]D. J. Hilton, R. D. Averitt, C. A. Meserole, G. L. Fisher, D. J. Funk, and A. J. Taylor, in *Quantum Electronics and Laser Science Conference, 2005. QELS '05*, Vol. 1 (The Optical Society of America, San Diego, CA, 2005), pp. 347–349.
[80]C. Stamm, N. Pontius, T. Kachel, M. Wietstruk, and H. A. Dürr, Phys. Rev. B **81**, 104425 (2010).
[81]D. Cheskis, A. Porat, L. Szapiro, O. Potashnik, and S. Bar-Ad, Phys. Rev. B **72**, 014437 (2005).
[82]A. Weber, F. Pressacco, S. Günther, E. Mancini, P. M. Oppeneer, and C. H. Back, Phys. Rev. B **84**, 132412 (2011).
[83]F. Dalla Longa, Ph.D. thesis, Eindhoven University, 2008, http://alexandria.tue.nl/extra2/200810818.pdf.
[84]A. J. Schellekens and B. Koopmans, *Abstract FC-13, 12th Joint MMM/Internag Conference, Chicago*, 2013.
[85]S. V. Halilov, A. Y. Perlov, P. M. Oppeneer, and H. Eschrig, Europhys. Lett. **39**, 91 (1997).
[86]S. V. Halilov, H. Eschrig, A. Y. Perlov, and P. M. Oppeneer, Phys. Rev. B **58**, 293 (1998).
[87]S. Essert and H. C. Schneider, J. Appl. Phys. **111**, 07C514 (2012).